

AN EXPERIMENTAL STUDY OF THE PERFORMANCE OF CRYSTAL MONOCHROMATORS ON  
PULSED NEUTRON SOURCES

C J Carlile, R Cywinski, V Wagner\*, R C Ward and W G Williams

Neutron Division, Rutherford Appleton Laboratory

\* Physikalisch-Technische Bundesanstalt, Braunschweig, Federal Republic of  
Germany

Abstract

An experimental programme carried out over the past 3-4 years and aimed at assessing the performances of single crystals as monochromators in a pulsed neutron source direct geometry spectrometer is described. As well as discussing the experience gained with a mock-up instrument we present measurements on a) the effect of cooling copper monochromators, b) crystal reflectivities, c) in-plane or horizontal focussing, and d) coherent resonance scattering of eV energy neutrons.

## 1. Introduction

In previous reports (1,2) we examined the feasibility of using crystal monochromators in a direct geometry inelastic scattering spectrometer on a pulsed neutron source. The principle of a stationary monochromator illuminating a scattering sample which is out of the direct beam offers some advantages over the use of a rotating chopper. These advantages include:

- (i) the elimination of the complex electronic and mechanical frequency and phasing units required by a chopper, a problem which is compounded if the neutron source is not absolutely periodic, and
- (ii) the possibility that a crystal spectrometer geometry may give lower backgrounds.

Although a cold neutron pulsed source crystal spectrometer has been built at the Tohoku Linac (3), no experimental data exists for an equivalent thermal or epithermal instrument. In this paper we describe the first tests of such a pulsed source spectrometer which were carried out at the Harwell electron linac. Our initial experience led us to make a more detailed examination of other aspects of using crystal monochromators in a direct geometry pulsed source instrument: the deleterious effect of simultaneous reflections; the effect of cooling crystals; the intensity gains in focussing geometries; and the possibility of using resonance scattering to enhance the monochromatic fluxes in the epithermal neutron region. The results of these investigations are also included in this paper.

## 2. Test Spectrometer

A schematic diagram of the experimental layout at the pulsed neutron source HELIOS at Harwell is shown in Figure 1. It was used to examine a copper monochromating crystal which was placed in a cryostat at 7.6m from the moderator.

The first tests were aimed at characterising the monochromatic beam and for these the copper crystal was oriented such that the diffracted beam from the [420] family of planes could be examined. Measurements in this geometry were carried out at temperatures of 260K, 107K and 15K. The

results are shown in Figure 2. At 260K three orders of reflection can be seen, with neutron energies ranging from 250 meV for the 420 reflection to 2.2 eV for the 12,6,0. Decreasing the temperature results in a marked increase in the integrated intensities of the Bragg peaks as illustrated in Figure 3. At the lower temperatures the 16,8,0 reflection at 4.0 eV is also clearly visible. The relative intensities of all the 420 orders at all temperatures were found to be in qualitative agreement with the theory of Popovici and Gelberg (4). The increase in Bragg intensity towards lower temperatures is mirrored by a decrease of the thermal diffuse scattering (TDS) background between the Bragg peaks. However at low temperatures, the rate of increase of Bragg intensity and decrease of TDS is limited by zero point motion; the rate of change of these quantities between 260K and 107K is greater than that between 107K and 15K. At 107K the contributions to the TDS from zero point motion and classical motion are approximately equal.

It is apparent from our results that a copper monochromator on a pulsed source crystal spectrometer should be cooled to at least 100K: a gain in intensity of 40% in the 420 reflection at 250 meV and 110% in the 840 reflection at 1 eV was observed on reducing the temperature from 260K to 15K with a consequent reduction in the background level between the peaks of ~ 30%. Cooling the crystal thus increases the signal to background by a factor of between 2 and 3.

The test spectrometer was then used to measure the inelastic scattering spectrum from zirconium hydride. This material exhibits a sharp optical vibration at 140 meV which has been used by Harling (5) and subsequently other workers to characterise inelastic scattering spectrometers. A 25% scattering sample of  $ZrH_2$  powder in an aluminium can was placed at the sample position in transmission geometry. At a  $30^\circ$  scattering angle the cross section for single phonon scattering with  $E_0 \sim 250$  meV is close to a maximum. The copper monochromator was first aligned to provide the 420 reflection at  $E_0 = 250$  meV and maintained at 15K. The data from a 48 hour run is shown in Figure 4. The monochromator was then reset to the 200 reflection. Using the second order 400 reflection at an energy of 200 meV a further 48 hour spectrum from  $ZrH_2$  was collected; this is shown in Figure 5. The data converted to double differential cross sections on an energy scale are shown in the insets to the figures. While the inelastic

mode measured with the lower incident energy is fully resolved, the scattered beam flight path of 1m is too short to resolve fully the equivalent elastic and inelastic features observed in the experiment using the higher incident energy.

The presence of the monochromator in the incident beam increased the background at the sample position by a factor of 4 at higher energies ( $\sim 10$  eV) and 2 at lower energies ( $\sim 200$  meV). However the background levels at the detector bank remained constant when either the monochromator was misaligned or when the scattering sample was removed. A comparison of the energy dependence of the background at the two positions indicated that, whilst the epithermal component at the sample was reproduced exactly at the detector bank, the Maxwellian component seen at the sample was absent at the detector bank. These observations indicated that the background level at the detector did not arise from the monochromatic beam falling on the sample. Instead it was concluded that the major part of the background at the detector bank could be attributed to the direct scattering (multiple Bragg and incoherent) of epithermal neutrons in the incident beam by the monochromator. Whilst the shielding around the experimental set-up was adequate against thermal neutrons it was relatively weak for epithermal neutrons. In particular the area of the shielding channel around the monochromatic beam was  $\sim 30$  times greater than the sample area. It is evident that in a properly engineered instrument great care is essential in the design of the shielding around the monochromator, the monochromatic beam and the sample position.

### 3. Crystal Reflectivities

In the experiments described in Section 2 no attempt was made to measure absolute reflectivities and only relative peak intensities were used in evaluating the data. The absolute reflectivities of copper monochromators were determined using reactor measurements at the PTB Braunschweig (6), and the effect on reflectivity of beam losses due to simultaneous reflections was investigated at the Harwell electron linac.

#### 3.1 Reactor Measurements

Integrated reflectivities  $R_0$  from two selected homogeneous copper monochromators in transmission geometry were obtained for the 331

reflection and its higher orders. The measurements were carried out on the S3 neutron diffractometer at the 1 MW research reactor at the PTB Braunschweig using neutron energies up to 1.08 eV. The incident spectrum from the graphite monochromator was determined by time of flight techniques in order to assign the proportion of neutrons in the incident beam belonging to each of the orders reflected from the graphite. The experimentally determined values of the integrated reflectivity  $R_\theta$  for two crystals of FWHM mosaic spread 1.8' and 4.8' (as determined by  $\gamma$ -ray diffraction) are summarised in Figure 6. Also shown are the calculated values of  $R_\theta$  from the theory of Popovici and Gelberg (4). The mosaic widths  $\beta$  of these crystals were determined by  $\gamma$ -ray diffractometry and, together with the  $R_\theta$  values, this allowed the peak reflectivities  $r_p$  to be obtained. These are also shown for the two crystals in Figure 6 as a function of neutron energy.

The experimental values of  $R_\theta$  are lower than the theoretical estimates by up to 50%. Geometrical arguments such as inhomogeneous illumination of the copper crystal or deviations of the mosaic distribution from the ideal situation could account for a certain proportion of this discrepancy. However, it seems that the main reason for the difference between theory and experiment is the loss of neutrons in the reflected beam due to competing Bragg reflections being partially satisfied.

### 3.2 Pulsed Source Experiments

White beam time of flight investigations into the efficiency of the monochromators were carried out on the Harwell electron linac pulsed neutron source. Again two crystals were selected for the measurements; the crystal of mosaic spread 4.8' previously used at the PTB and a further crystal of mosaic spread 5.7'. Both crystals were aligned on goniometers with their  $\langle 116 \rangle$  direction along the goniometer axis using the Badger neutron diffractometer on the DIDO reactor at AERE Harwell before transferring to the 3-circle sample table of the Linac High Symmetry Spectrometer.

Measurements were made in transmission geometry of the 331 and higher order reflections from the 4.8' crystal and also of the beam transmitted through the crystal. The transmitted beam spectrum is

shown in Figure 7 and reveals the presence of a series of reflections taking place at different times of flight,  $t$ , proportional to  $d \sin \theta$ .

Transmission measurements using the white beam time of flight technique can give precise information on the effect of simultaneous reflections in degrading the efficiency of selection of the required monochromatic beam, provided the instrumental resolution is sufficiently good. In particular by rotating the crystal about the scattering vector, not only can the fluctuation in intensity in the reflected beam be followed, but the transmitted beam gives direct information on the reflections contributing to this degradation. This type of "Renninger Scan" was carried out by Kuich and Rauch (7) in order to maximise the intensities available from the monochromator on a reactor-based spectrometer. Their conclusion was that intensity gains of  $\sim 25\%$  were obtainable at low incident energies whereas no gain was possible at higher incident energies ( $> 100$  meV). However, the apparent gain in reflected intensity using this technique is highly dependent on the instrumental resolution.

Kuich and Rauch's data in fact indicates that losses through parasitic reflections are equally bad at high energies for all orientations of the crystal about the scattering vector on a poor resolution spectrometer. This is illustrated in Figure 8 where Ewald spheres for high incident energies and low incident energies are shown. It is evident that the higher energy Ewald sphere has a higher probability of intersecting more than one reciprocal lattice point than the lower energy sphere. At high energies it is practically impossible to avoid simultaneous Bragg reflections even with a high resolution instrument since the vertical collimation is generally relaxed to  $\sim 1^\circ$  in order to increase the neutron current at the sample.

Transmission measurements on the 5.7' mosaic spread crystal carried out in parallel with reflection measurements indicated experimentally the importance of properly taking the effect into account. The crystal was aligned with its  $\langle 100 \rangle$  direction along the scattering vector in transmission geometry and its  $\langle 011 \rangle$  direction perpendicular to the scattering plane. Reflections up to the 4th order were observed at a neutron energy of 1.31 eV. In the transmitted beam (Figure 9) the dips in the transmission due to the  $(2n \ 0 \ 0)$

reflections are evident together with numerous simultaneous reflections at different wavelengths. The 200 reflection is contaminated in the long time wing by a neighbouring reflection with a similar value of  $d \sin \theta$ . Rotating the crystal about the scattering vector in  $5^\circ$  steps, as shown in curves 2, 3 and 4 of Figure 9 greatly varies the extent to which this reflection is degraded by simultaneous reflections. Figure 6 shows that the experimentally determined  $R_\theta$  values for the 1.8' mosaic spread crystal are closer to the theoretical values at low incident energies than for the 4.8' mosaic spread crystal where the discrepancy remains significant. This trend is consistent with the hypothesis outlined above.

#### 4. In-plane (Horizontal) Focussing

The use of focussing techniques to increase the fluxes at the scattering sample in continuous source instruments is well-known (8). Both vertical (out-of-plane) and horizontal (in-plane) focussing are in principle possible using multi-component monochromators, and together these can give order of magnitude gains in sample fluxes. We have recently studied the application of focussing for pulsed source spectrometers (9) and have demonstrated the feasibility of horizontal focussing. The method of vertical focussing on a pulsed source, though not demonstrated, is the same as that at a continuous source, since it simply involves a vertical extension of the monochromator array. Horizontal focussing cannot be achieved however by the accepted continuous source techniques because of the correlation between wavelength and time-of-flight on a pulsed source.

The principle of horizontal focussing on a pulsed source is shown in Figure 10. P is the point of intersection of a perpendicular from the focal point (sample position) to the incident neutron beam line.  $L_1$  and  $l_0$  are the distances to P from the moderator and focal point, respectively. Time focussing at the sample occurs when the term:

$$d_{hkl} \sin \theta_{hkl} [L_1 + l_0 \tan \theta_{hkl}]$$

is arranged to be equal for a set of monochromators  $M_1, M_2, M_3 \dots$  etc placed after each other. It can be shown that acceptable values of the wavelength spread and angular divergences of the incident beam can be achieved by using reflections from planes with progressively narrower

d-spacings as the distance from the moderator is increased. In practice this is most easily done by using higher order Bragg reflections from one type of crystal monochromator.

The feasibility of the method has been demonstrated using two copper monochromators cut so that they reflected from their [400] and [420] planes respectively. The measurements were performed on a four-circle diffractometer at the Harwell electron linac pulsed source. The important geometric parameters in these tests are listed in Table 1.

$L_1$	11.17 m
$l_0$	0.79 m
Moderator - 1st monochromator	11.17 m
Monochromator separation	17.1 cm
$\theta_B$ for 1st Monochromator [Cu(400)]	45°
$\theta_B$ for 2nd Monochromator [Cu(420)]	51.1°
Angular Spread at Focus	12.2°
Monochromator 1 Wavelength	1.278 Å
Monochromator 2 Wavelength	1.258 Å
Wavelength Spread	0.020 Å

Table 1. Geometric Parameters in Horizontal Focussing Tests.

Figs 11(a) and 11(b) show the diffraction patterns obtained with the first and then the second crystals aligned. Note that the 200 reflection occurs at a longer time than the recorded time frame and does not appear. Only the higher order reflections from this plane are observed. The 420 and its orders are observed in the second pattern. Figure 11(c) shows the pattern obtained with both crystals aligned. The 400 and 420 reflections are coincident in time as are the 800 and 840 reflections. The 600 reflection from the first monochromator stands alone as does the 10,0,0. Figure 11(d) shows the effect of a slight misalignment of the second monochromator where the superimposed diffraction peaks of the previous pattern are now split.



Experimental limitations unfortunately did not allow us to measure the attenuation of the incident beam by the first crystal. We were therefore not able to evaluate the intensity of the beam falling onto the second crystal nor consequently to quantify the overall intensity gain of a focussing monochromator array compared to a single monochromator. However we can estimate this gain by using published single crystal cross-sections (10). Thus at a wavelength of 1.27 Å, as used in these tests, a gain of ~ 1.7 in intensity over a single monochromator could be expected. For a possible five crystal array at a wavelength of 0.74 Å (energy = 150 meV) the overall gain would be a factor of ~ 3.2.

In conclusion we have demonstrated a method for horizontal focussing on a pulsed neutron source using a wavelength of 1.27 Å. The angular spread of the monochromatic beam and its wavelength spread are acceptable for incoherent scattering spectroscopy. At shorter neutron wavelengths more crystals can be assembled in the monochromator array whilst still maintaining acceptable values of the wavelength and angular spreads. For example for a wavelength of 0.74 Å ( $E_0 \sim 150$  meV) five sets of copper monochromators reflecting from the [444] planes up to the [731] planes and within a space of 20 cms along the incident beam would reflect a monochromated beam whose wavelength varies only by 0.01 Å and whose angular range is 12°. At longer neutron wavelengths it is possible to produce sets of alloy monochromators (Cu-Ge for example) with a range of lattice parameters which are able to fulfill the conditions described above. Overall gains in the intensity of the monochromated beam from this technique should approach a factor of three over a single monochromator. As this increase can also be achieved with vertical focussing (8) a properly designed two-dimensional monochromator array on a pulsed neutron source would produce intensity gains of an order of magnitude over a single-crystal monochromator.

## 5. Resonance Scattering in Epithermal Neutron Crystal Monochromators

Brugger (11) was the first to suggest combining the effects of coherent Bragg diffraction with the enhanced scattering lengths which occur at nuclear resonances to produce a crystal monochromator suitable for use at resonance energies in the 1-10 eV range. Tests of this idea have now been carried out on the Harwell linac pulsed source at a neutron energy of 6.67 eV using a single crystal of uranium dioxide (12). Although coherent

resonance scattering was observed in these measurements (Figure 12) it was also evident that the benefit of the enhanced scattering in a practical crystal was lost due to the much higher absorption cross-section at the resonance maximum. The scattering cross-section at the peak of the 6.67 eV resonance in uranium-238 is approximately 1198 barns  $\text{at}^{-1}$  which is a factor  $\sim 20$  lower than the absorption cross-section. This means, as was pointed out by Brugger, that the effective crystal thickness for diffraction purposes is only  $\sim 50 \mu\text{m}$ . In order to produce a viable electron volt energy crystal monochromator using this principle a higher scattering to absorption cross-section is needed. Since this only occurs for nuclear resonances at much higher energies ( $\gtrsim 100 \text{ eV}$ ), when the Debye-Waller factor is prohibitively high for coherent reflections, we conclude that it is unlikely that a practical monochromator can be produced for the 1-10 eV region using this technique.

## 6. Summary

A series of experimental measurements relevant to the design and construction of a direct geometry crystal monochromator spectrometer on a pulsed neutron source has been performed. Data has been collected on crystal reflectivities, a horizontally focussed arrangement of two crystals, and the effect of coherent resonance scattering for eV energy neutrons has been examined. In addition a test crystal spectrometer has been built and used to show the advantage of cooling copper monochromators, as well as to provide first inelastic spectra for downscattering from the epithermal energy region.

The case for building a crystal spectrometer depends critically on the comparison of its performance relative to a chopper spectrometer. In parallel with the experimental programme described several comparisons of the performances of these two types of direct geometry spectrometer have been made (2), and in the latest (13) it is concluded that the chopper spectrometer is superior at all neutron energies higher than about 50 meV. The main reason for the poorer performance of crystals is the difficulty of providing full illumination in a practical geometry, rather than any deficiency due to the factors discussed in this paper. The measurements we have described are however important in optimising the design of a low energy crystal spectrometer, especially the effect of focussing.

## References

1. C J Carlile and W G Williams, Rutherford Laboratory Report RL-81-028 (1981).
2. C J Carlile and W G Williams, Rutherford Laboratory Internal Report NDR/P6/83 (1983).
3. N Watanabe, Y Ishikawa and K Tsuzuki, Nucl Instrum and Meth 120 (1974) 293.
4. M Popovici and D Gelberg, Nucl Instrum and Meth 40 (1966) 697.
5. O K Harling, Rev Sci Instrum 37 (1966) 697.
6. C J Carlile, W G Williams and V Wagner, Physikalisch-Technische Bundesanstalt Report PTB-FMRB-104 (1984).
7. G Kuich and H Rauch, Nukleonik 9 (1967) 139.
8. R Scherm and V Wagner, Neutron Inelastic Scattering, IAEA Vienna (1978) 149.
9. C J Carlile and R C Ward, J Appl Cryst 18 (1985) 16.
10. A K Freund, Nucl Instrum and Meth 213 (1983) 495.
11. R M Brugger, unpublished (1983).
12. C J Carlile, R C Ward and B T M Willis, J Appl Cryst, in press.
13. C J Carlile, A D Taylor and W G Williams, Rutherford Appleton Laboratory Report RAL-85-052 (1985).

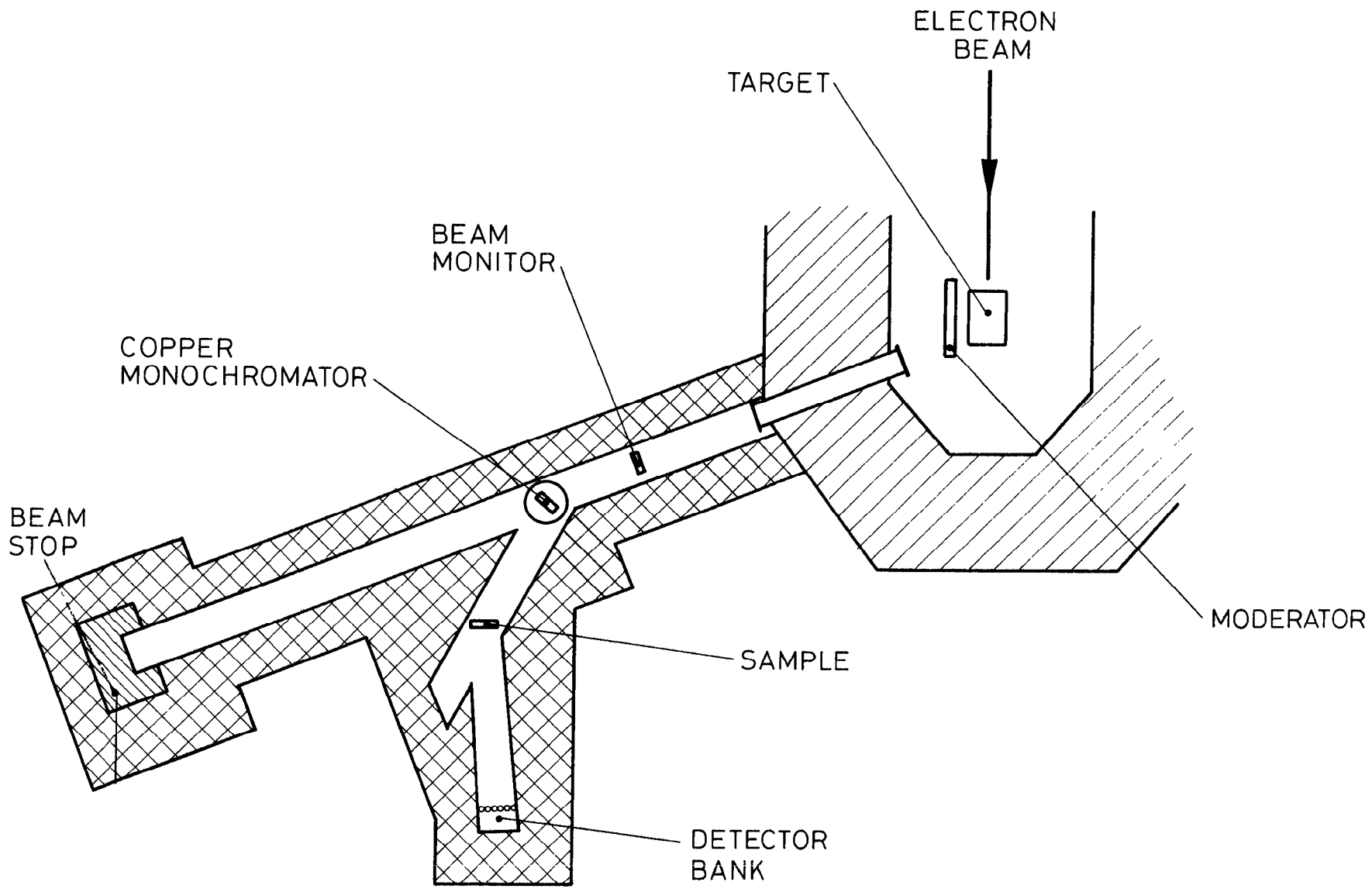


Figure 1. Test crystal spectrometer layout at the Harwell linac pulsed neutron source.

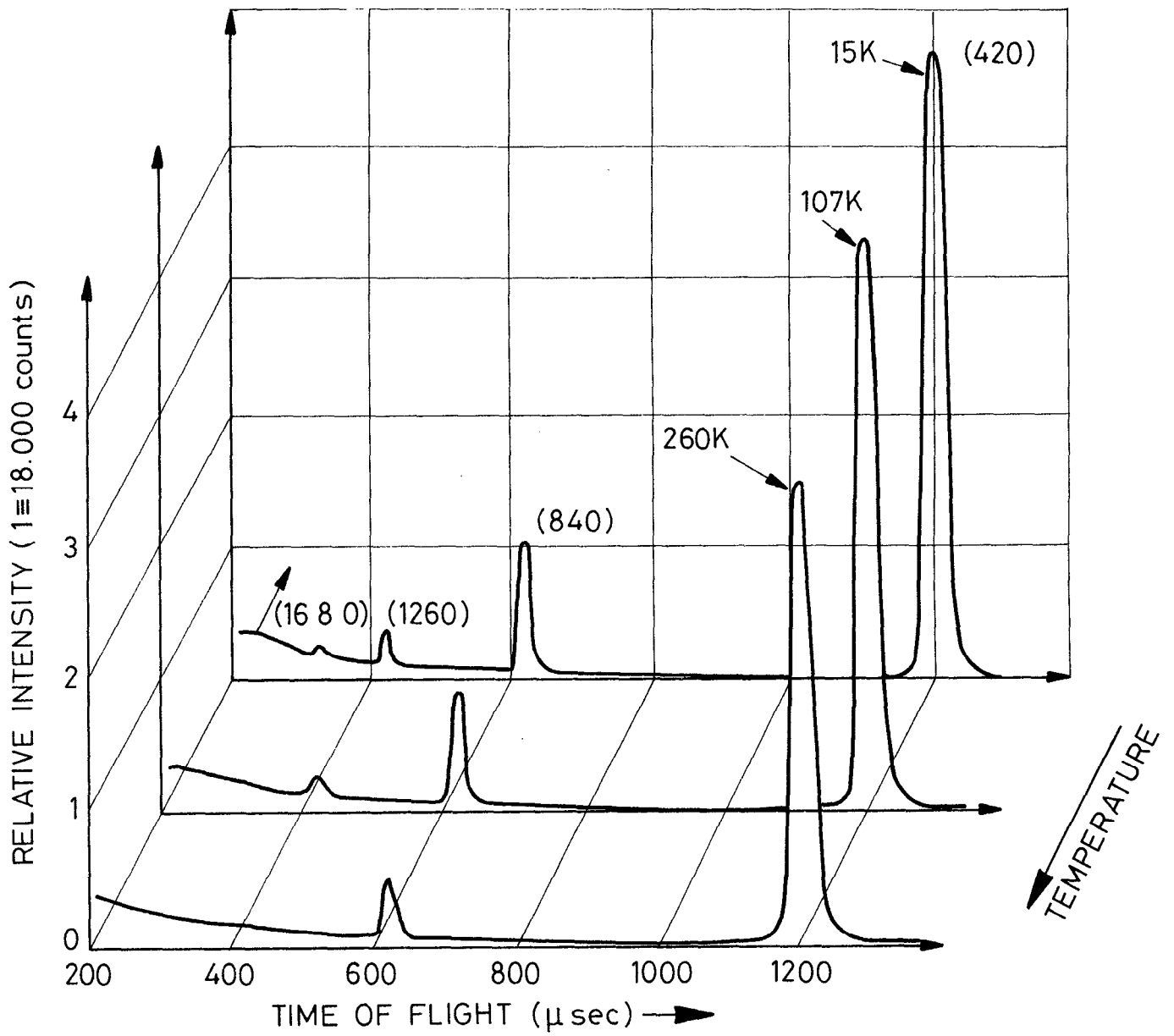


Figure 2. Diffraction peaks from the Cu [420] family of planes at different temperatures.

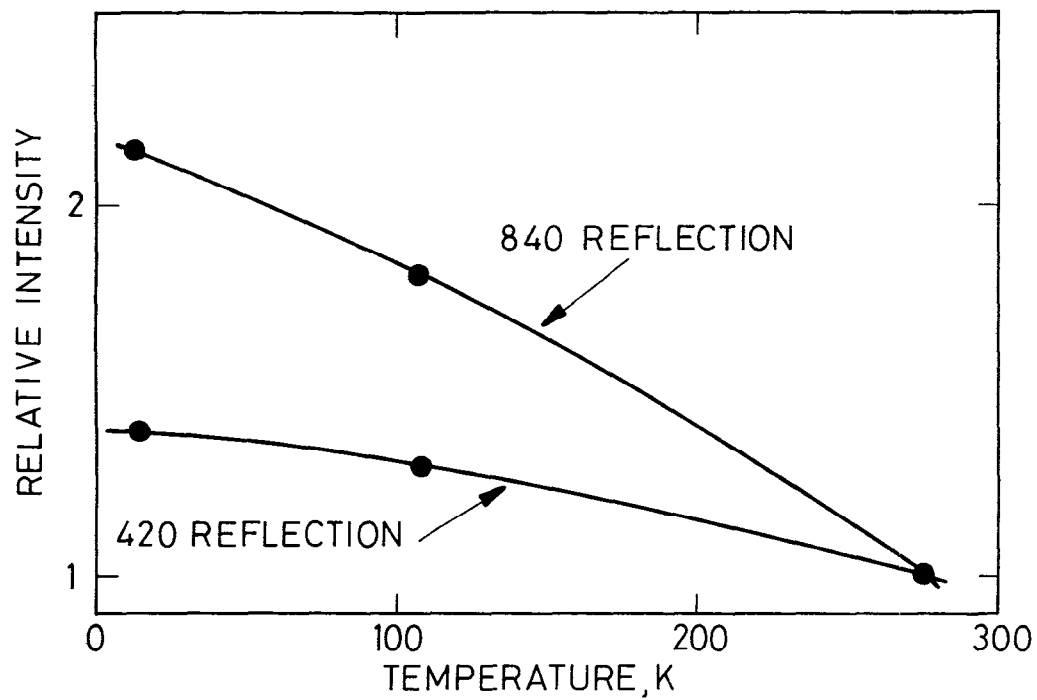


Figure 3. Relative peak intensities of Figure 2 normalised to values at 260K.

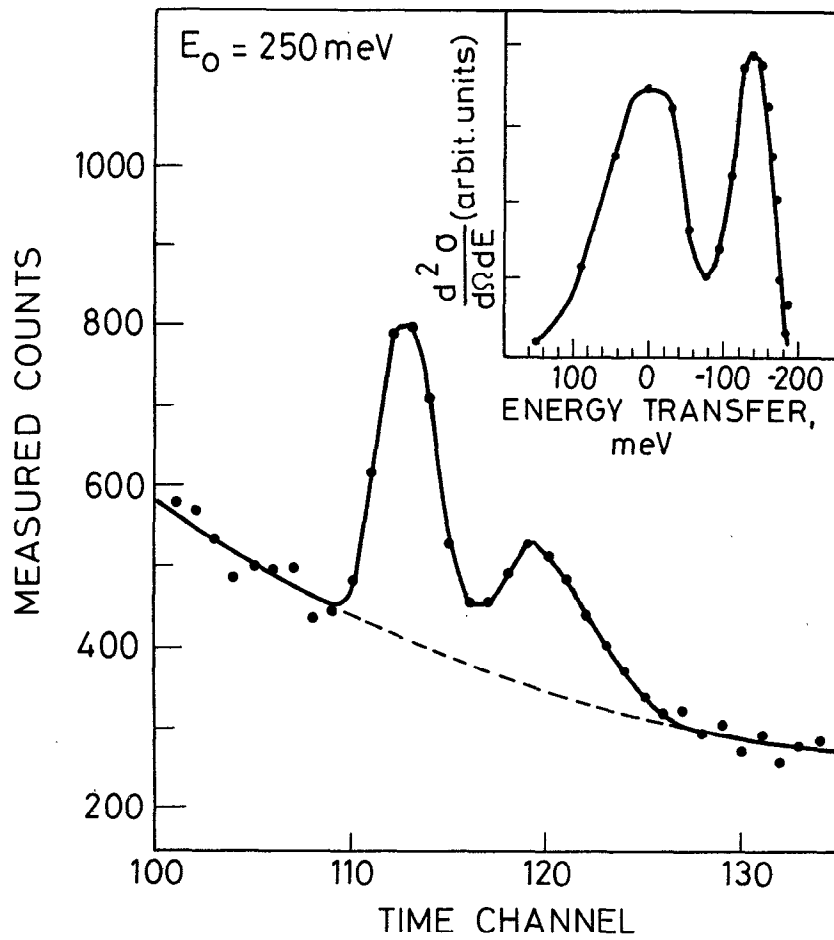


Figure 4. Inelastic spectra from  $ZrH_2$  observed with the test spectrometer with incident energy  $E_0 = 250$  meV.

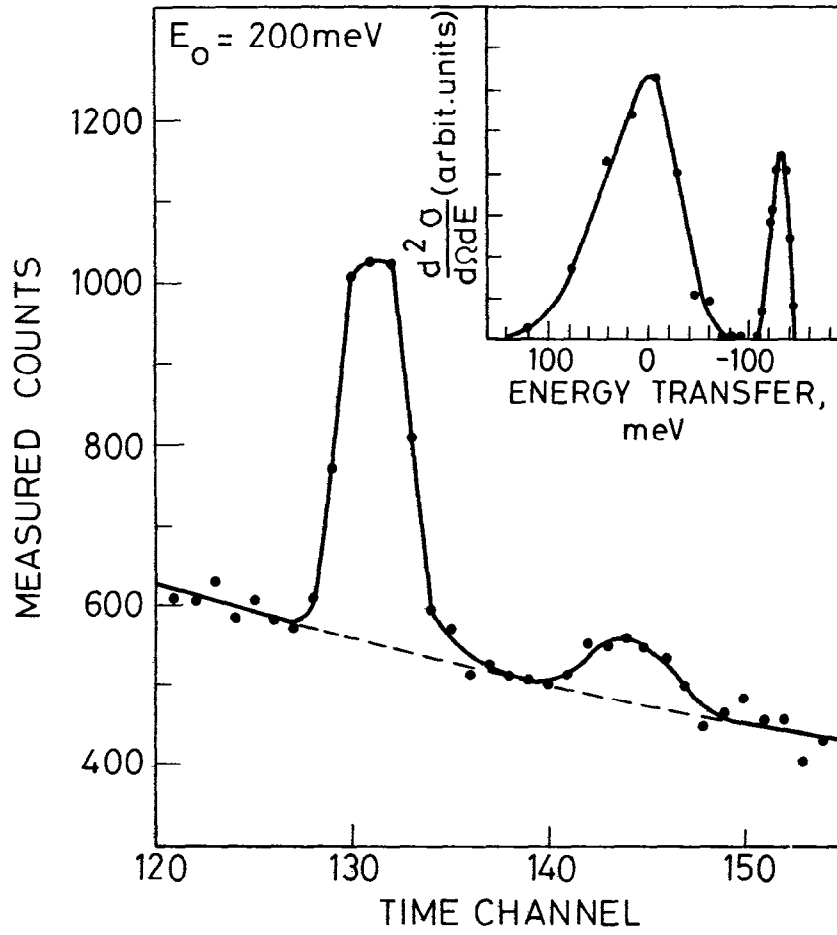


Figure 5. As Figure 4 with incident energy  $E_0 = 200$  meV.



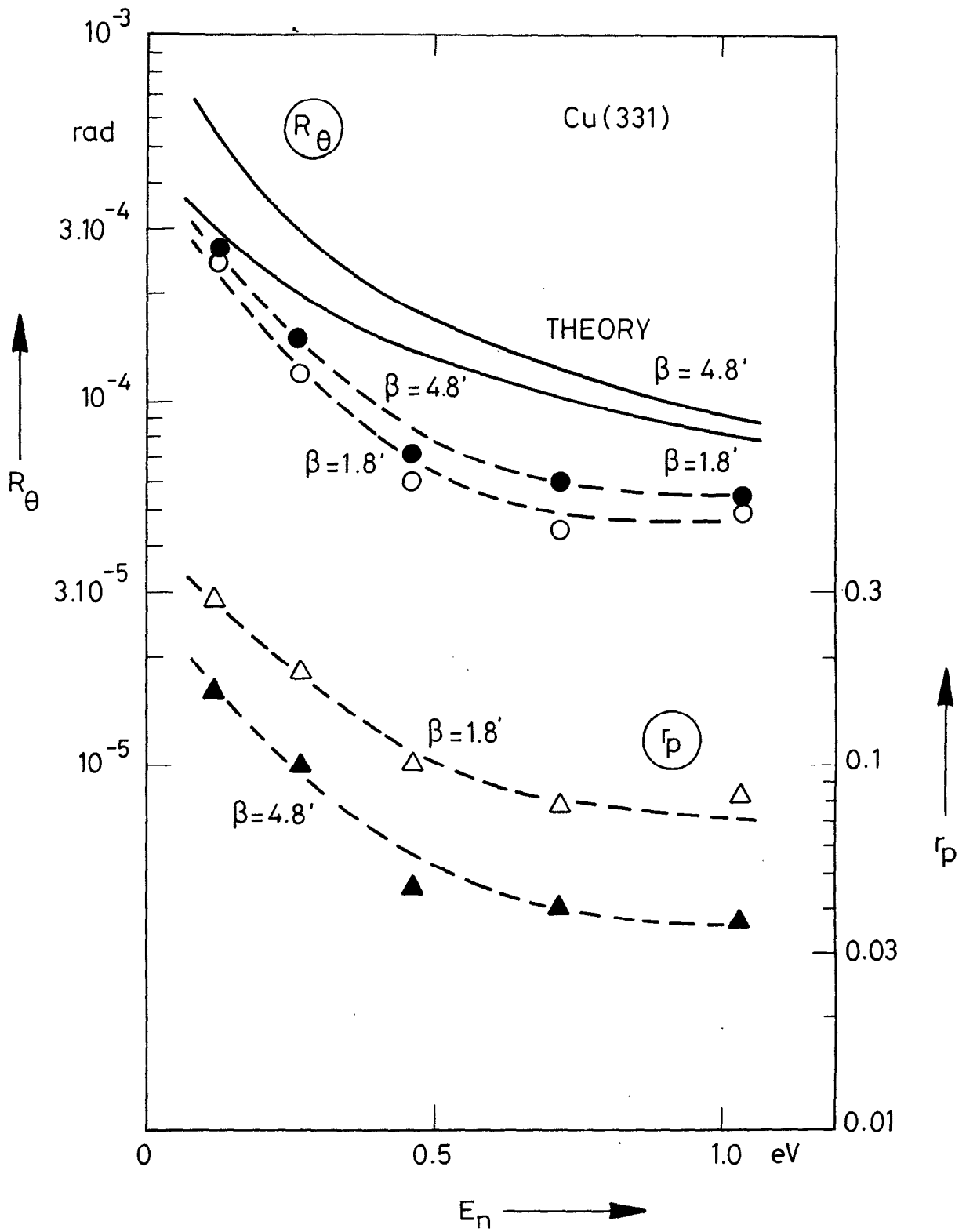


Figure 6. Integral reflectivity  $R_\theta$  and peak reflectivity  $r_p$  as function of neutron energy  $E_n$  for two copper crystals. FWHM of the mosaic distributions are  $\beta = 4.8'$  and  $\beta = 1.8'$ .

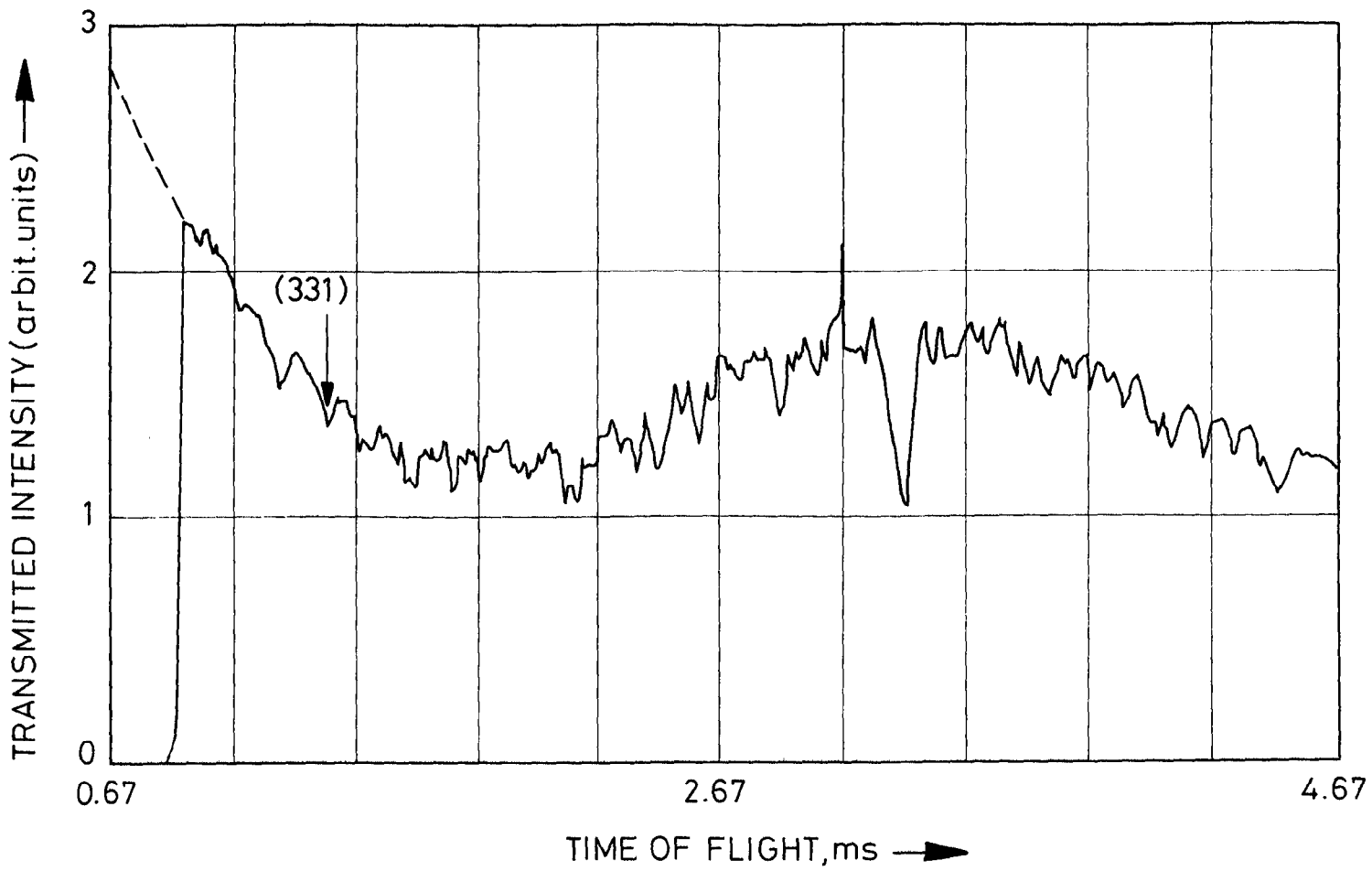


Figure 7. Time-of-flight spectrum of the transmitted beam of a Cu crystal with  $\beta = 4.8^\circ$  set for a 331 reflection.

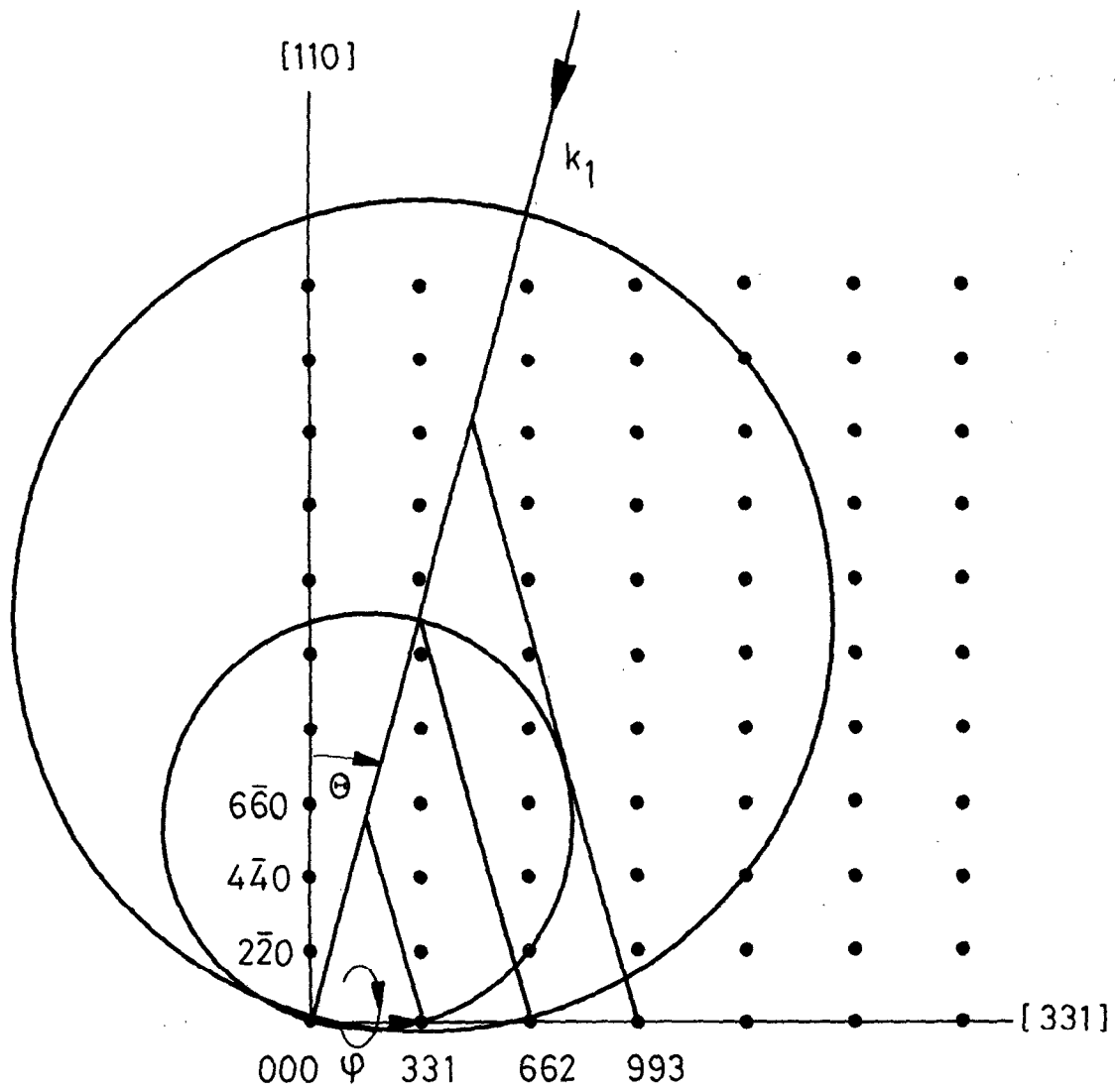


Figure 8. Section of the scattering plane (i.e. the  $[11\bar{6}]$  plane) with the reciprocal space showing the Ewald spheres for different incident energies.

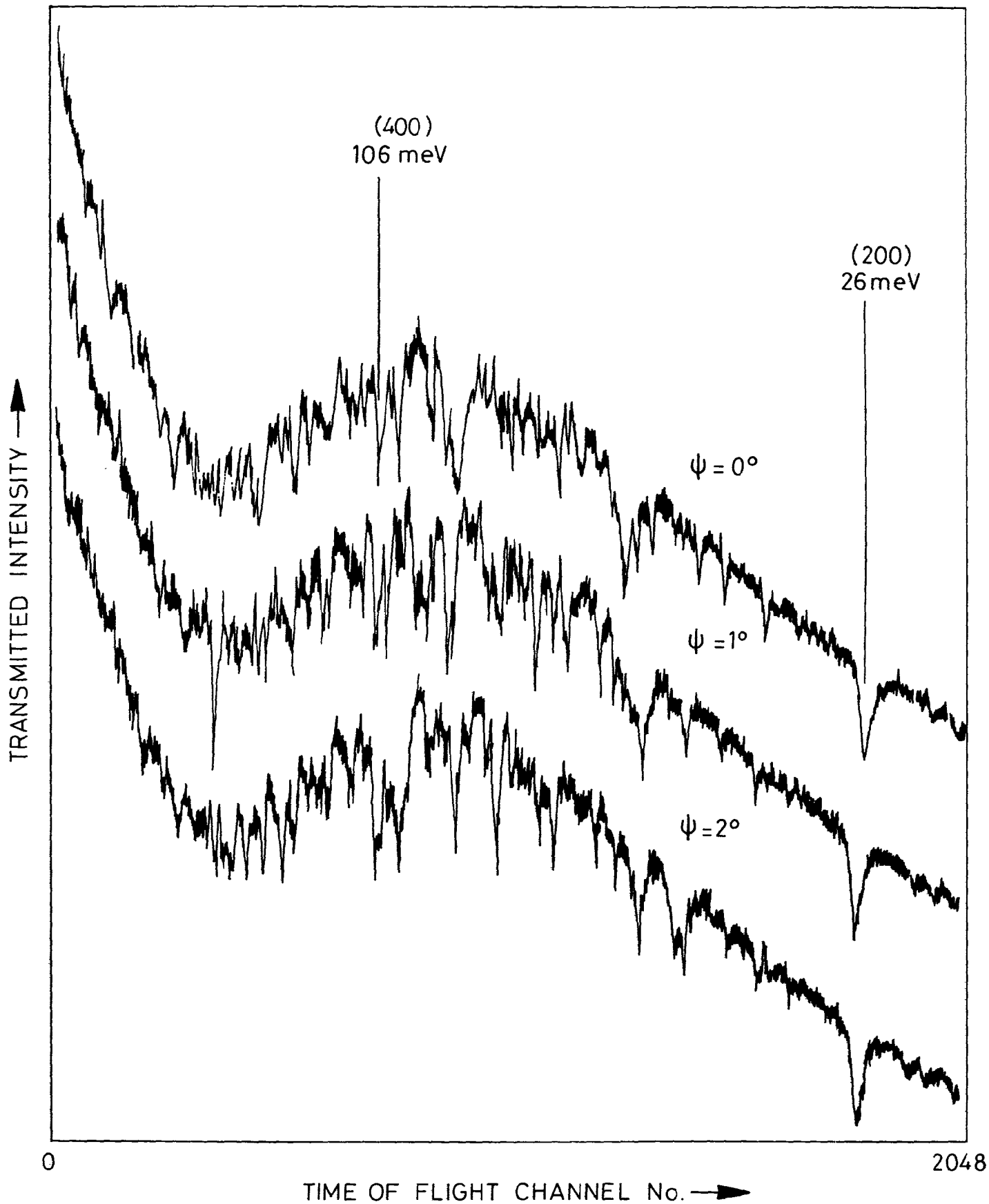


Figure 9. Time-of-flight spectrum of the transmitted beam of a Cu crystal with  $\beta = 5.8'$  set for the 200 reflection.  $\psi$  denotes the rotation around the scattering vector. For  $\psi = 0$  the  $\langle 011 \rangle$  axis of the crystal is vertical.

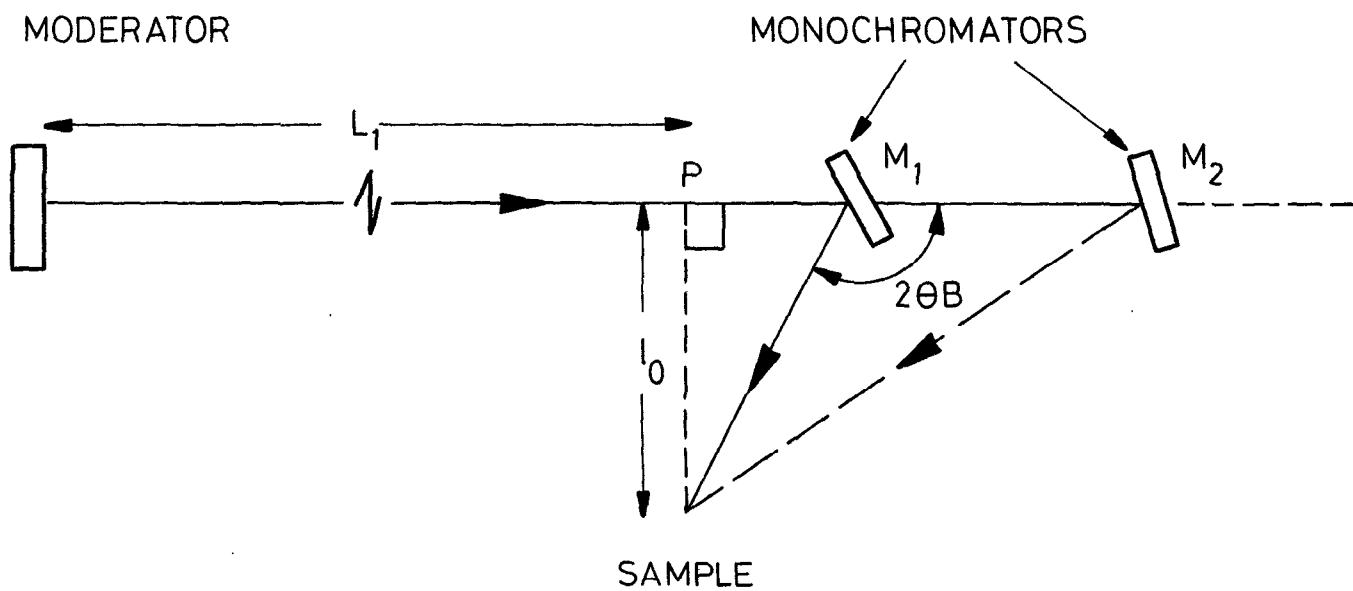


Figure 10. Principle of horizontal focussing using two crystal monochromators on a pulsed neutron source.

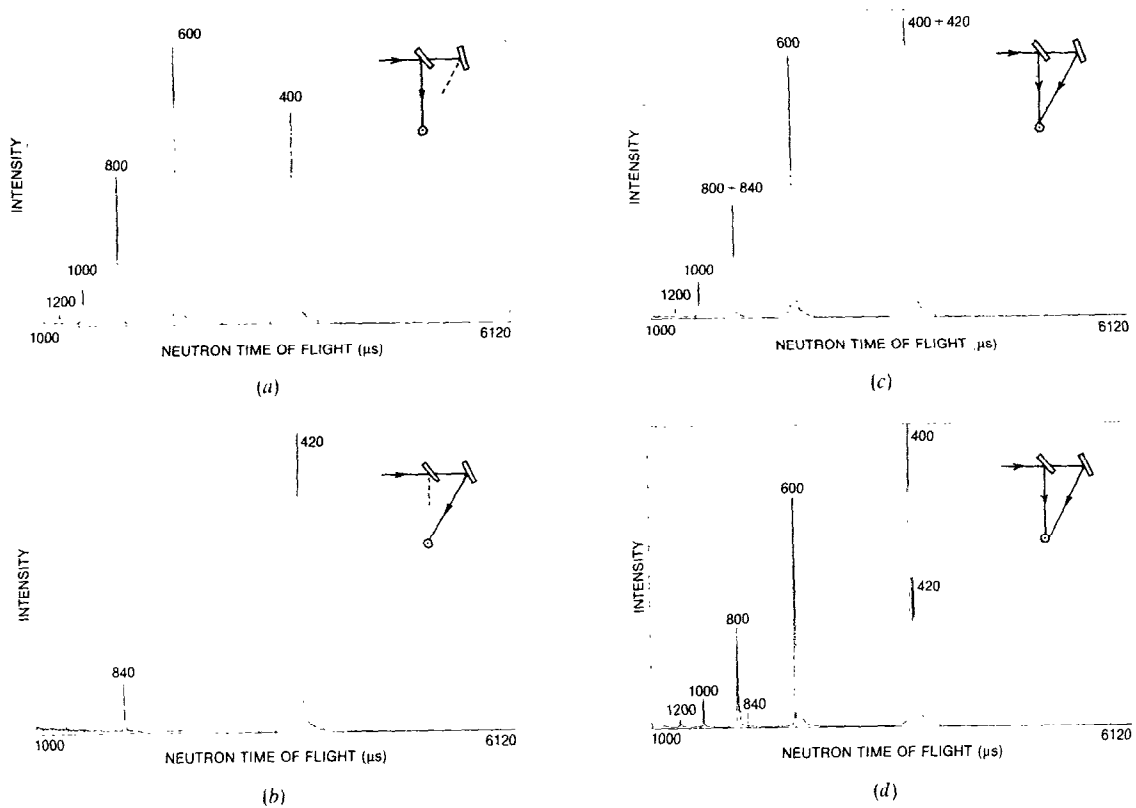


Figure 11. Observed diffraction patterns uncorrected for the incident beam spectrum and detector efficiency. Both crystals were copper, the first aligned with the  $\langle 200 \rangle$  direction along the scattering vector, the second aligned with the  $\langle 210 \rangle$  direction along the scattering vector. The  $hkl$  values of each reflection are as indicated. (a) The pattern with crystal 1 aligned and crystal 2 misaligned with the 400 and higher orders reflecting. (b) The pattern with crystal 1 misaligned and crystal 2 aligned. The 420 and 840 are visible. (c) The resultant pattern with both crystals aligned. (d) The effect of a slight misalignment of one of the crystals.

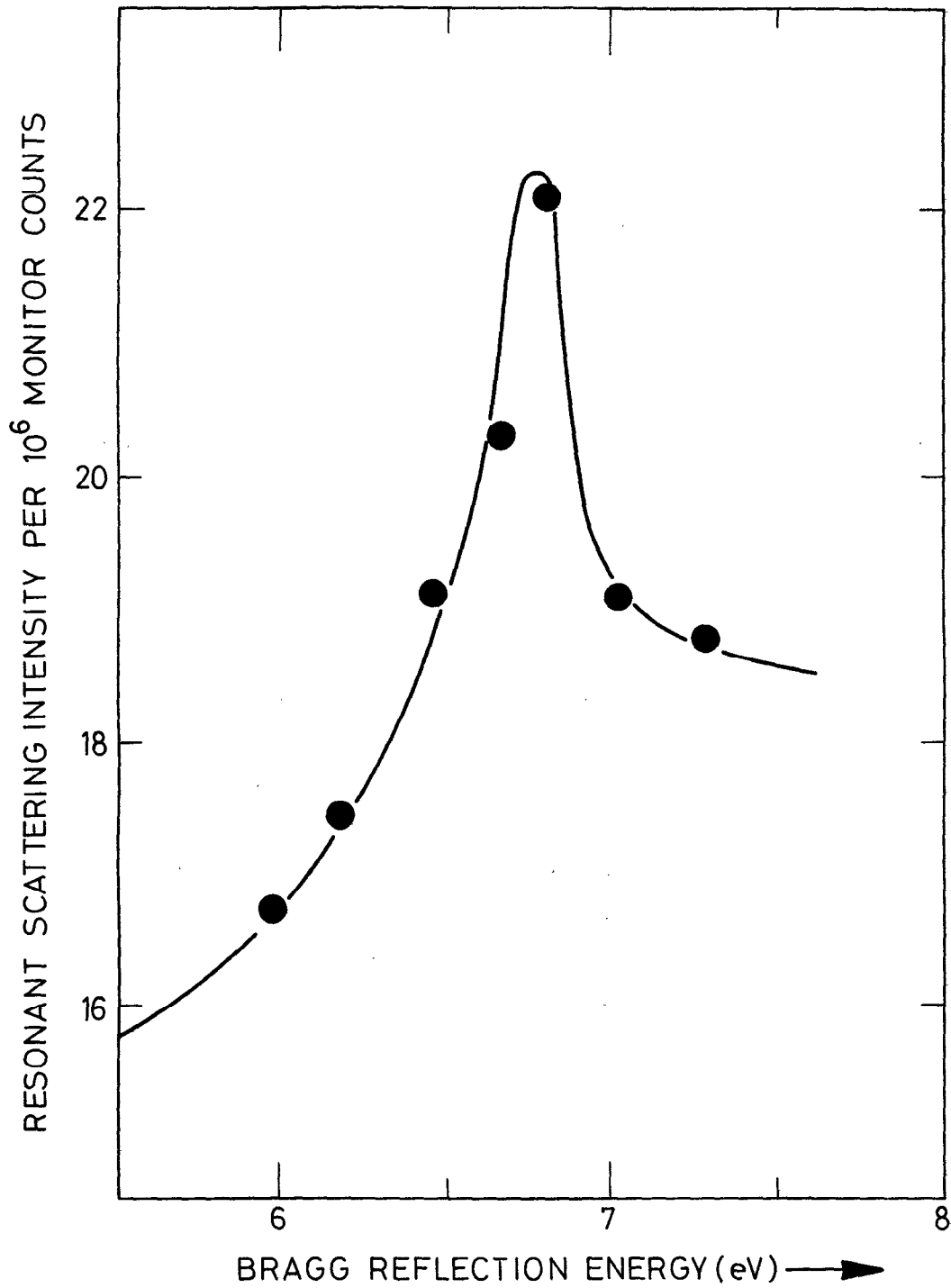


Figure 12. The integrated intensity recorded at the 6.67 eV resonance in uranium as the 18,6,0 Bragg reflection from  $\text{UO}_2$  is scanned through the resonance energy. The scattered intensity is normalised to the incident beam intensity and the full line is a guide to the eye.